

 Open access • Journal Article • DOI:10.1080/00102209208951821

## Structure of Reacting and Non-Reacting Swirling Air-Assisted Sprays — [Source link](#)

Vince McDonell, M. Adachi, G. S. Samuelsen

**Institutions:** University of California, Irvine

**Published on:** 01 Jan 1992 - Combustion Science and Technology (Taylor & Francis Group)

**Topics:** Flow velocity

Related papers:

- [Structure of reacting and nonreacting, nonswirling, air-assisted sprays, part ii: drop behavior](#)
- [Structure of a particle-laden round jet](#)
- [Group Combustion of Liquid Droplets](#)
- [Spark-ignited spherical flames propagating in a suspended droplet cloud](#)
- [Structure of a Swirl-stabilized, Combusting Spray](#)

Share this paper:    

View more about this paper here: <https://typeset.io/papers/structure-of-reacting-and-non-reacting-swirling-air-assisted-x8ph4r9sus>

# UC Irvine

## UC Irvine Previously Published Works

### Title

STRUCTURE OF REACTING AND NONREACTING SWIRLING AIR-ASSISTED SPRAYS

### Permalink

<https://escholarship.org/uc/item/7hx3s184>

### Journal

COMBUSTION SCIENCE AND TECHNOLOGY, 82(1-6)

### ISSN

0010-2202

### Authors

MCDONELL, VG  
ADACHI, M  
SAMUELSEN, GS

### Publication Date

1992

### DOI

10.1080/00102209208951821

### Copyright Information

This work is made available under the terms of a Creative Commons Attribution License, available at <https://creativecommons.org/licenses/by/4.0/>

Peer reviewed

## Structure of Reacting and Non-Reacting Swirling Air-Assisted Sprays

V. G. MCDONELL, M. ADACHI\* and G. S. SAMUELSEN *UCI Combustion Laboratory, University of California, Irvine, CA 92717, U.S.A.*

**Abstract**—A detailed characterization of a methanol spray produced by an air-assist atomizer with swirling atomizing air has been conducted. This study is the third of a series which examines the structure of sprays produced by a standardized atomizer which can be operated in three modes, pressure swirl, non-swirling air-assist, and swirling air-assist. Measurements of drop size and three components of velocity, three components of the gas phase velocity, the concentration of hydrocarbons within the spray, and time resolved droplet measurements are obtained at axial locations of 7.5, 15, 25, 35, 50, 75, and 100 mm. These measurements are obtained for both reacting and non-reacting cases. In addition, the atomizing air flow in the absence of the spray is characterized. Primary observations from the present study are that (1) the presence of the drops alters the structure of the gas phase turbulence, including the degree of isotropy, (2) the presence of reaction strongly impacts the axial and radial velocity components, while having little impact on the azimuthal component, (3) reaction reduces the mean diameter of the distributions at all locations, (4) a strong dependence of the axial and radial velocity upon drop size exists, whereas little dependency is observed for the azimuthal component, and (5) detailed examination of the droplet arrival indicates clustering of drops. Finally, it is observed that the findings from the present study both agree and contradict with the results of others. This is indicative of the inherent complexity of reacting sprays, and suggests that a more methodical approach to studying the impact of swirl and geometrical changes is required to understand the effects of atomizing air, swirl, vaporization, and phase interaction such as that undertaken in the present effort.

### 1 INTRODUCTION

Detailed studies of droplet behavior in spray flames are necessary to (1) develop understanding of the physical processes of evaporation, fuel-air mixing, and transport phenomena, and (2) provide additional data for further development and verification of numerical codes. Such information is required to continue the current efforts to (1) mitigate environmental impact and (2) enhance performance and efficiency of liquid-fueled continuous combustion systems. Unfortunately, the spray combustion problem is confounded by the presence of many interdependencies. It is difficult to separate the effects of vaporization, combustion, transport, and phase interaction on the resulting drop size and velocity distributions. Also, typical specification of an atomizer (diffraction based line of sight SMD, cone angle, and flow number) can lead to two atomizers which are identical based upon these parameters, but are significantly different in the detailed structure of the spray. As a result, the present study was undertaken to examine the structure of sprays produced by a *standardized* atomizer which is capable of operating in a pressure swirl or air-assist mode.

This paper presents results from the third part of a series of experiments directed at better understanding the behavior of sprays, both reacting and non-reacting. The first two parts provide results from a non-reacting pressure atomized spray (McDonell and Samuelsen, 1991a), and reacting and non-reacting, non-swirling, air-assist sprays (McDonell, Adachi, and Samuelsen, 1991a, b).

The objectives of the current paper are to provide (1) better understanding of sprays produced by swirling air-assist atomizers, (2) a detailed data base suitable for model verification and development, and (3) provide a detailed study against which other

\*Visiting Scientist, Horiba Ltd.

studies may be compared. In support of the third objective, Table I provides details from studies which provide spatially resolved measurements in reacting and non-reacting sprays. The information provided in these studies is used in an effort to summarize current understanding about spray flames and their relationship to the non-reacting case.

## 2 EXPERIMENT

The facility used in the present study is the same as described elsewhere (McDonell and Samuelsen, 1991a; McDonell and Samuelsen, 1991b). Briefly, the spray is injected downwards in the center of a square duct which is 457 mm on a side. Three degrees of freedom are provided to the atomizer via a traverse system. The optical diagnostics remain in place. Two-component phase Doppler interferometry (PDI) is used to measure the drop size and velocities along with the velocity of the gas phase, and infrared extinction/scattering (IRES) is used to measure the concentration of vapor within the spray. Both instruments, as used in the present study, are described in detail elsewhere (Bachalo and Houser, 1984; McDonell and Samuelsen, 1991a; Adachi, McDonell and Samuelsen, 1991).

The downfired arrangement is used to retain flow field characteristics which were used to help stabilize the reaction in the non-swirling cases previously examined (McDonell *et al.*, 1991a, b).

## 3 RESULTS

The results are presented in two sections, gas phase behavior and droplet behavior. In each case, reacting and non-reacting sprays are considered. In addition, the behavior of the single phase flow is considered within the gas phase results to provide a baseline against which the gas phase behavior in the presence of the spray can be compared. To orient the reader, Figure 1 presents photographs of the spray under non-reacting and reacting conditions.

The photographs reveal important changes in the overall structure of the spray which are caused by the presence of reaction. These changes include (1) a reduction in the axial extent of the spray due to evaporation and consumption of the drops and (2) a "U-shaped" void of drops which is associated with the location of the reaction zone. This picture is consistent with group combustion theory (Chiu and Liu, 1977), which indicates that, for a group combustion number,  $G \gg 1$ , a sheath of reaction will surround a cloud of droplets. Note that this structure is similar to that observed previously in twin-fluid atomizer spray flames (*e.g.*, Mao *et al.*, 1986; McDonell *et al.*, 1991b; McDonell and Samuelsen, 1991b).

### 3.1 Gas Phase Behavior

**3.1.1 Gas phase velocities** Figures 2–8 present a comparison of the gas phase mean and fluctuating velocities for (1) the single phase flow, (2) the gas in the presence of non-reacting spray, and (3) the gas in the presence of the reacting spray.

At the nearest axial location,  $Z = 7.5$  mm, an on-axis recirculation zone is observed for all three cases, as indicated by the radial profile of the mean axial velocity,  $U$ , shown in Figure 2. The presence of spray reduces the strength of this recirculation zone due to the axial momentum in the streamwise direction of the drops. The gas in

the presence of the non-reacting spray shows a consistently higher value of  $U$  along the centerline which is again attributed to the phase interaction which tends to reduce the strength of the recirculation zone. Near the edge of the spray, at axial locations downstream of the atomizer, the presence of the non-reacting drops narrows the spread of the gas jet.

The impact of reaction is seen starting at  $Z = 25$  mm, where the heat release causes an acceleration of the gas, resulting in an increase in  $U$  when compared to the non-reacting case. Note that the expansion is greater away from the centerline, suggesting that greater heat release is occurring in those regions.

Radial profiles of the mean radial velocities,  $V$ , for the three cases are presented in Figure 3. The presence of the non-reacting drops reduces and shifts radially the location of the maximum radial velocity at  $Z = 7.5$  mm. This is attributed to the "prompt" atomization action associated with this atomizer, where a strong jet of air blasts a sheet of liquid. The presence of the liquid sheet tends to reduce the spread of the gas jet, which is consistent with the behavior of the axial velocity.

The presence of reaction causes a significant increase in the radial velocity, which is again due to the heat release and subsequent expansion of the gas phase. By  $Z = 100$  mm, the radial expansion has subsided, and the difference between the reacting and non-reacting cases is less.


Figure 4 presents radial profiles of the mean azimuthal velocity,  $W$ , for the three cases. Unlike  $U$  and  $V$ ,  $W$  is not strongly affected by the presence of the drops for either non-reacting or reacting conditions. The differences observed are within the experimental error of the measurement. An explanation is that the only source of swirl in the three cases is the atomizing air which has high momentum only near centerline where the presence of small drops has little impact. In the reacting case, symmetry dictates that the flow cannot expand in a preferred azimuthal direction, thus, reaction does not affect the mean azimuthal velocities of the gas phase. This is consistent with observations in an air-blast atomizer spray (McDonell and Samuelsen, 1991b).

The fluctuating axial, radial, and azimuthal gas phase velocities ( $u'$ ,  $v'$ , and  $w'$ ) are presented in Figures 5–7. The behavior of  $u'$  (Figure 5) suggests that the presence of the spray impacts the levels of fluctuations in the gas phase. This modulation has been observed previously in sprays (e.g., McDonell and Samuelsen, 1991b). In the present case, the level of  $u'$  are increased along the centerline at  $Z = 50$ , 75, and 100 mm, which is attributed to the mixing of drops of different sizes and velocities. This effect will be clarified in the section on drop behavior. Away from the centerline at  $Z = 50$ , 75, and 100 mm, an increase in  $u'$  at the edge of the reaction zone is observed. The location of the peak in  $u'$  for the reacting case corresponds to the location of the maximum in  $dU/dr$  at  $Z = 50$ , 75, and 100 mm. This is not so strongly observed in the single phase and non-reacting cases.

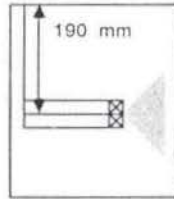
Radial profiles of  $v'$  are presented in Figure 6. Similar trends are observed for  $v'$  as for  $u'$ . However,  $v'$  does not show as much correlation with the mean flow gradients. Note that  $u'$  and  $v'$  appear similar in magnitude. One exception to this is in the reaction zone, where  $u'$  becomes significantly larger than  $v'$ . This indicates that the presence of reaction in the present case tends to reduce the levels of isotropy found in the gas phase. One explanation for this is that, in the axial direction, buoyancy acts against the general flow direction, resulting in greater instability of this velocity component.

Profiles of  $w'$ , shown in Figure 7, shows that the presence of drops tends to damp the turbulence near the atomizer. Farther downstream, however, no appreciable difference between the three cases is observed. The levels of  $w'$  are similar to those of  $v'$  and  $u'$ , with the exception of the levels of  $u'$  in the reaction zone, as mentioned

TABLE I  
Previous studies with spatially resolved measurements in reacting sprays

Reference	Geometry	Fuel type	Atomizer	Conditions	Measurements	Diagnostic
present study		Methanol	Swirling Air-Assist	$m_f = 1.26$ g/s $m_a = 1.29$ g/s Atomizing air only, reacting and non-reacting sprays Ambient temperature and pressure	$U_g, V_g, W_g,$ $U(D), V(D),$ $W(D)$ $D$ Volume Flux $D(t)$ [HC] $T$ $Z = 7.5, 15, 25$ 35, 50, 75, 100, 150 mm	2D PDI 2D PDI 2D PDI 2D PDI 2D PDI IRES Thermocouple
McDonell and Samuelsen, (1991b)	same as present study but with duct air at 1.0 m/s	Methanol	Air-Blast free of aerodynamic swirl	$m_f = 2.03$ g/s $m_a = 2.03$ g/s atomizing air only, reacting and non-reacting cases Ambient temperature and pressure	$U_g, W_g$ $U(D), W(D)$ $D$ Volume Flux $Z = 50, 75, 100$ mm	2D PDI for each case
McDonell, Adachi, and Samuelsen (1991a, b)	same as present study	Methanol	Non-swirling air-assist	$m_f = 1.26$ g/s $m_a = 1.29$ g/s Atomizing air only, reacting and non-reacting sprays Ambient temperature and pressure	$U_g, V_g, u'v'_g$ $U(D), V(D),$ $\theta_w(D)$ $D$ Volume Flux $D(t)$ [HC] $T$ $Z = 7.5, 15, 25,$ 35, 50, 75, 100, 150 mm	2D PDI 2D PDI 2D PDI 2D PDI IRES Thermocouple

Bachalo, Rudoff,  
and Sankar (1990)



Kerosene

Pressure Swirl  
with aerodynamic  
swirl

$m_f = 0.82 \text{ g/s}$   
 $m_a = 2208 \text{ g/s}$   
(total air flow)

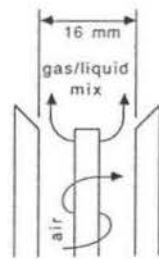
Reacting and  
Non-Reacting  
Sprays

Ambient  
temperature and  
pressure

$D$   
 $U(D, t)$   
 $Z = 80, 150,$   
 $200 \text{ mm}$

2D PDI for each  
case

Hardalupus,  
Taylor, and  
Whitelaw (1990)



Kerosene/  
Methane Mix

Gas/Liquid  
combination  
injector with  
aerodynamic swirl

$m_a = 6.30 \text{ g/s}$   
 $m_{\text{meth}} = 0.17 \text{ g/s}$   
 $m_f = 0.55, 0.96 \text{ g/s}$

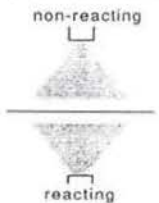
Reacting and  
Non-Reacting  
Sprays

Ambient  
temperature and  
pressure

$D$   
 $U(D), V(D),$   
 $W(D)$   
 $Z = 0.64, 4.8,$   
 $11.2, 19.5 \text{ mm}$

1D PDI in all cases

Mao, Wang, and  
Chigier (1986)



Kerosene

Swirling Air-Assist

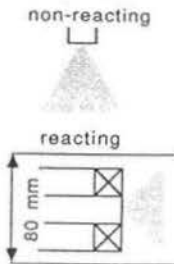
$m_f = 0.22 \text{ g/s}$   
 $m_a = 0.92 \text{ g/s}$

Reacting and  
non-reacting  
sprays

$D$   
 $U_d$   
 $N$   
 $Z = 10, 15, 35,$   
 $55, 75 \text{ mm}$

1D PDI in all cases

McDonnell, Wood,  
and Samuelsen  
(1986)



JP-4

Swirling Air-Assist  
with aerodynamic  
swirl

$m_f = 0.91 \text{ g/s}$   
 $m_a = 1.36 \text{ g/s}$

Non-reacting  
spray without  
aerodynamic swirl  
Reacting Spray  
within model  
combustor

Ambient  
temperatures and  
pressures

$D$   
 $U_d, W_d$   
 $U_e, W_e$   
 $T$   
 $Z = 20, 30, 40,$   
 $50 \text{ mm (spray)}$

1D PDI  
1D PDI  
LA  
Thermocouple



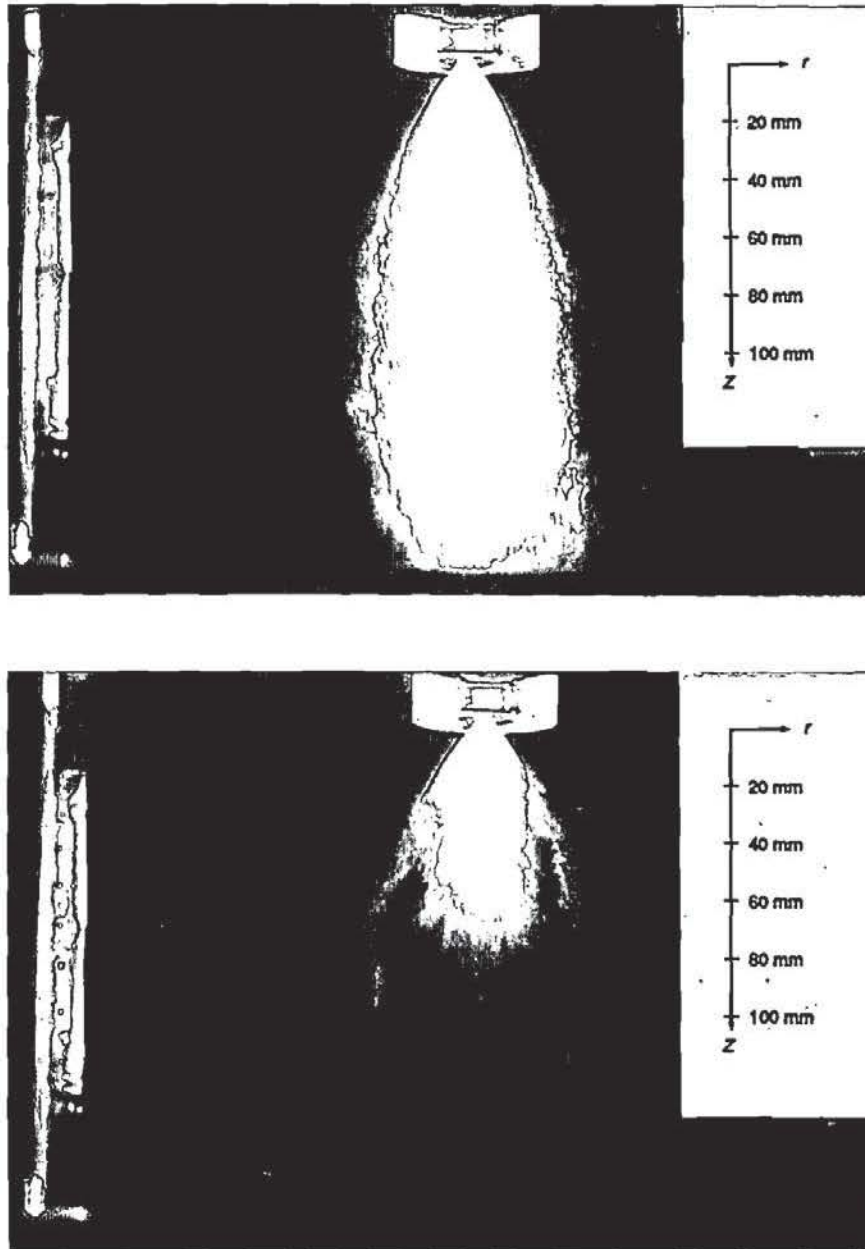
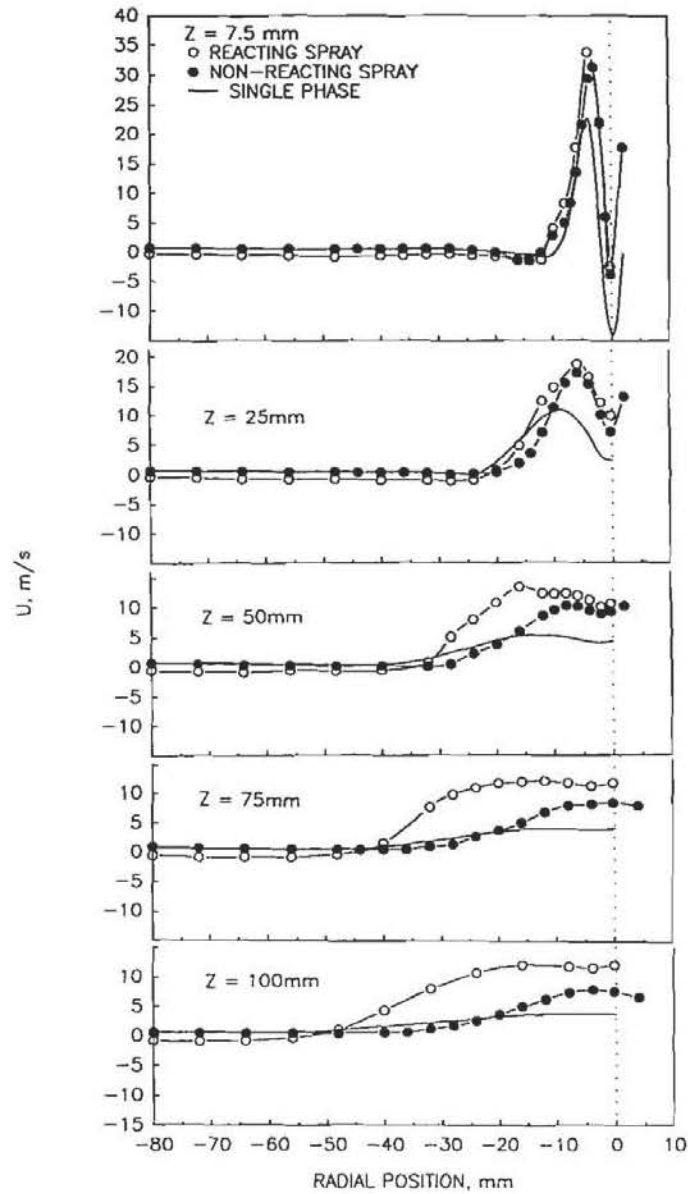


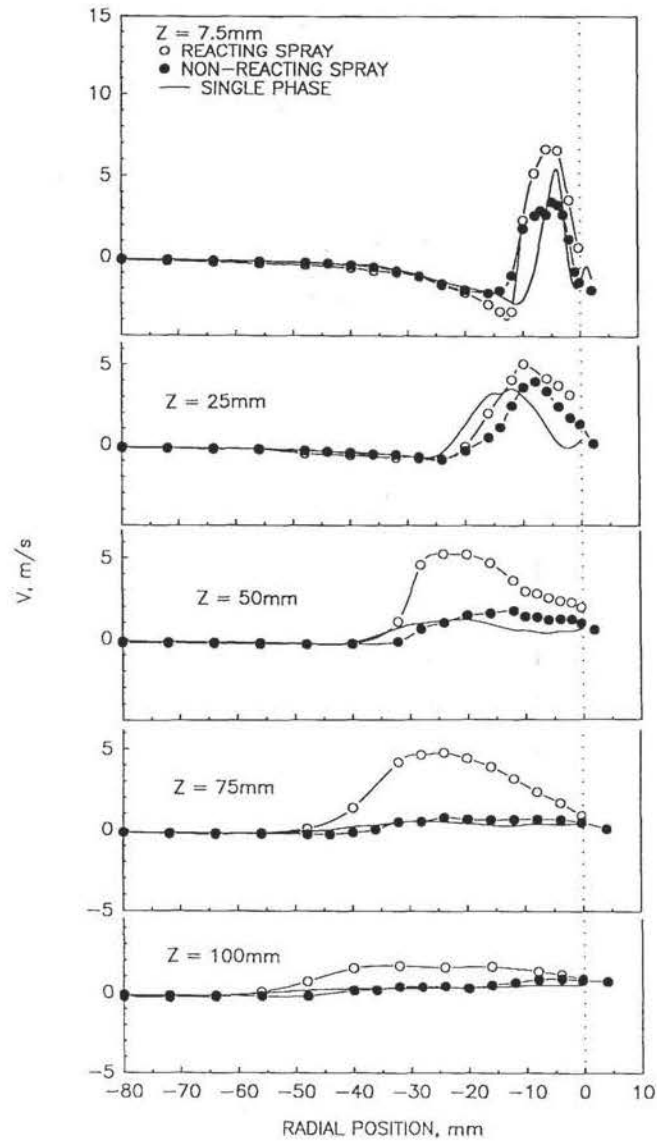
FIGURE 1 Photographs of spray structure. (a) Non-reacting, (b) reacting.



FIGURE 2 Radial profiles of  $U$ .

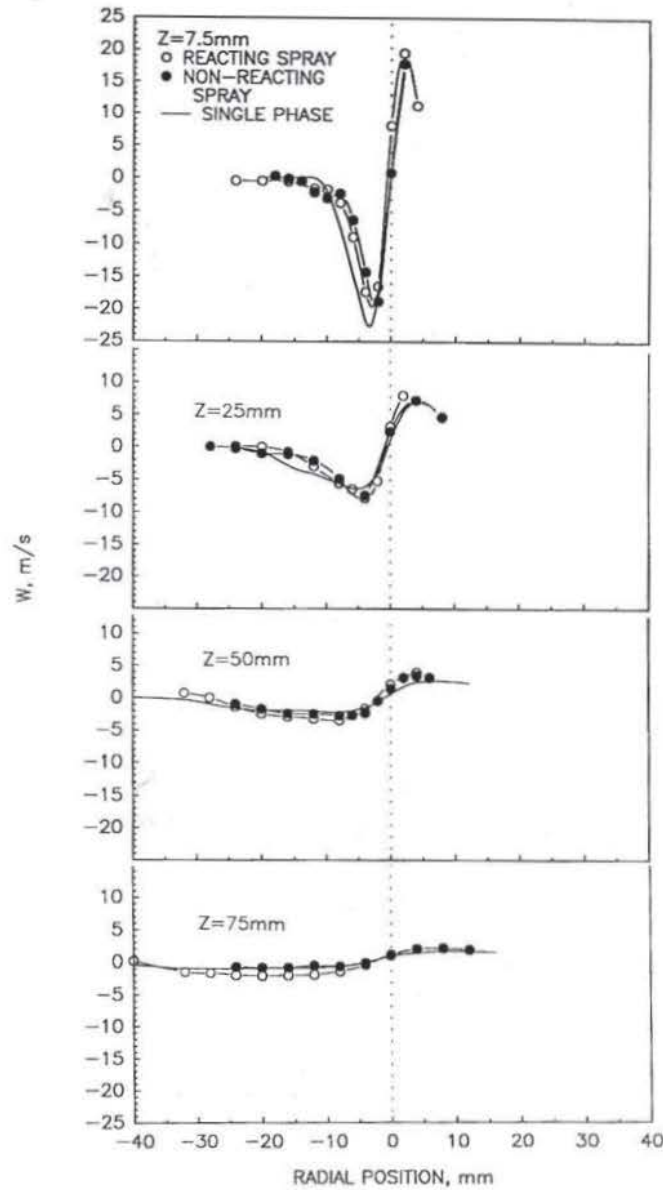
above. Noteworthy is the local peak in  $w'$  which can be observed at the centerline at  $Z = 7.5$  and 25 mm, especially in the single phase case. This may be associated with some unsteadiness in the flow (*e.g.*, precession of the vortex, "flapping").

In all the profiles of the fluctuating velocities at  $Z = 7.5$  mm, a secondary peak exists at radial locations,  $r$ , of  $-10$  to  $-12$  mm. This is attributed to the presence of drops in high numbers with large variation in velocity and high slip velocities, which generates turbulence in these regions.

FIGURE 3 Radial profiles of  $V$ .

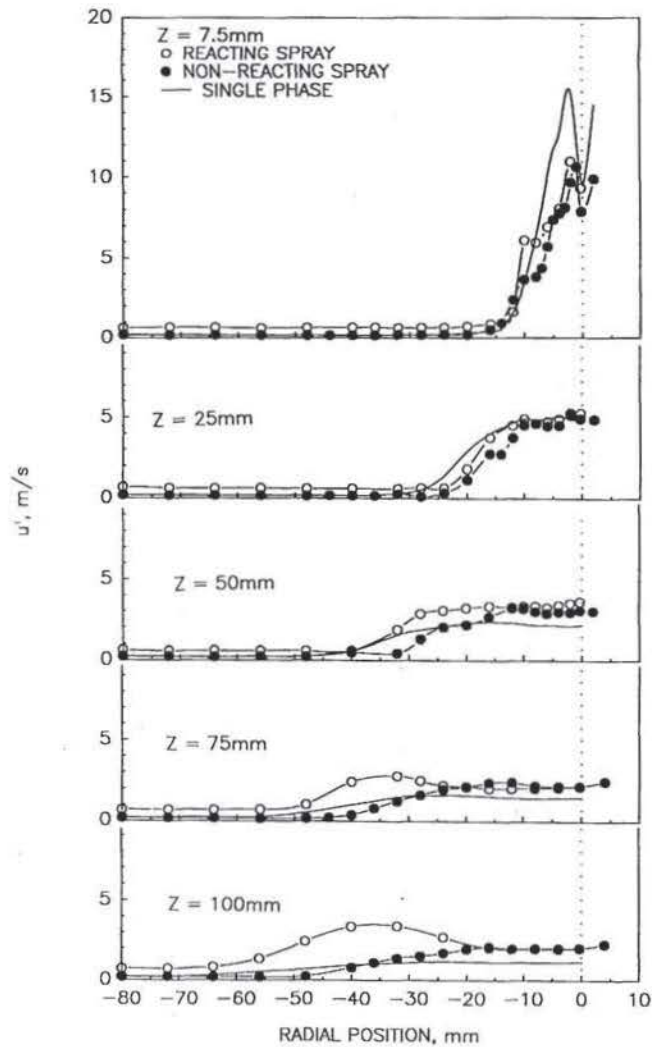
To better quantify the impact of the spray and reaction upon the isotropy of the turbulence of the gas phase, Figure 8 presents ratios of the components. For the single phase and non reacting cases,  $u'$  and  $w'$  retain similar levels. The presence of reaction causes a consistent increase in  $u'/w'$ , which is attributed to the downfired reaction and the expansion of gases axially. This same behavior has been observed in an air-blast spray (McDonell and Samuelsen, 1991b).

Comparing  $u'$  and  $v'$  shows that, near the centerline, similar levels occur for the single phase case and for the gas in the presence of the non-reacting spray. At radial

FIGURE 4 Radial profiles of  $W_r$ .

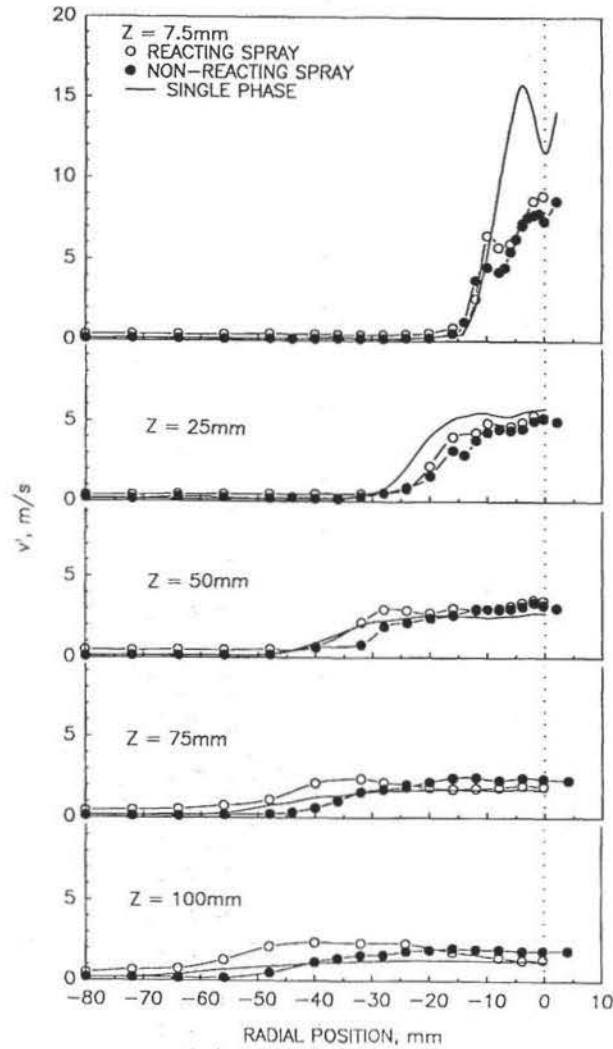
locations of 35 to 55 mm, a sharp drop in this ratio is observed for these two cases. Finally, in the outer region of the flow,  $u'$  is significantly higher than  $v'$  which is attributed to the nature of the turbulence in the co-flowing stream. The presence of reaction tends to raise the value of  $u'/v'$  at all locations relative to the non-reacting and single phase cases. In all cases, the turbulence is not isotropic.

3.1.2 *Methanol gas concentration* Figures 9 and 10 present contour plots of the

FIGURE 5 Radial profiles of  $u'$ .

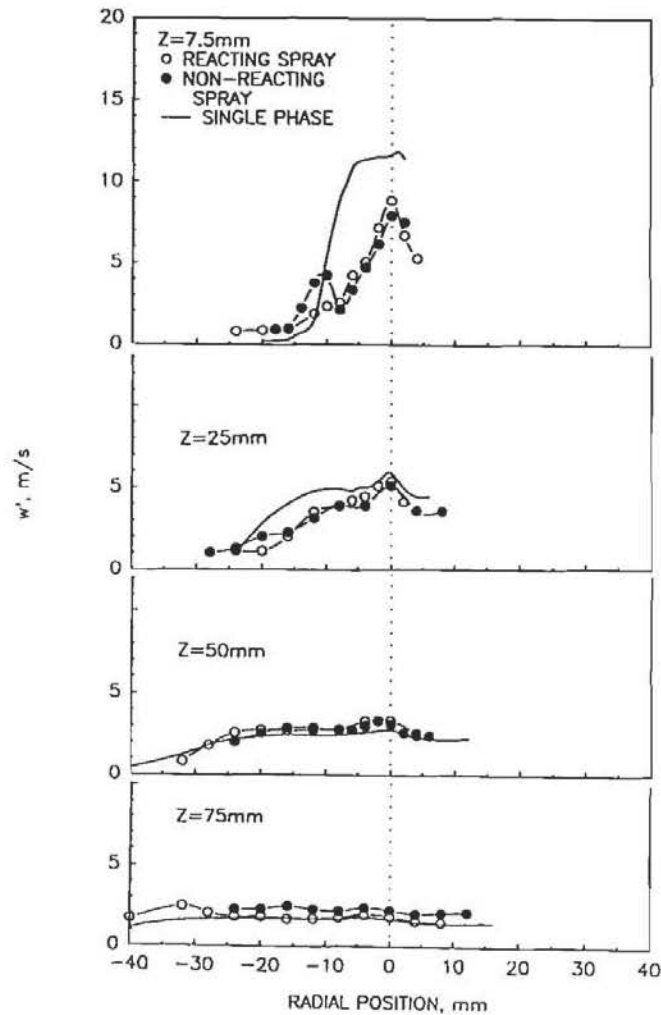
mean hydrocarbon concentration for the non-reacting and reacting cases overlaid upon velocity vectors for the gas phase velocity formed from the values of  $U$  and  $V$ . In addition, temperature contours are provided for the reacting case as measured using a thermocouple. In the region of the reacting case where appreciable numbers of drops are present, the thermocouple measurements are likely affected by impaction of drops, and must be considered qualitative. The origin in Figures 9 and 10 corresponds to the centerline at the exit plane of the atomizer, and is offset from the scaled injector schematic for clarity.

Figure 9 shows the results for the non-reacting case. Immediately downstream of the atomizer, along the centerline, the peak concentrations are observed. These concentrations correspond to an approximately saturated condition for the methanol vapor (McDonnell and Samuelsen, 1991a). This occurs despite the strong dilution

FIGURE 6 Radial profiles of  $v'$ .

associated with the atomizing air. The strong mixing which occurs downstream of the atomizer due to the presence of swirl in the atomizing air stream enables the vapor concentration to reach saturation levels measured. With increased axial distance from the atomizer, the dilution associated with entrained air combined with a reduction in saturation levels due to evaporative cooling of the air reduces the concentration of methanol vapor. The role of entrainment at the edge of the jet is shown by the vectors, which show significant flow of surrounding air towards the jet.

Figure 10 shows the same results for the reacting case. In this case, the heat release occurring in the downfired geometry results in recirculation of products in the outer regions of the flow. This heated flow mixes with incoming fresh air from above somewhere between 25 and 50 mm below the nozzle exit plane. Some of the recirculated products form the local "peninsula" of hydrocarbons which forms at the edge

FIGURE 7 Radial profiles of  $w'$ .

of the spray. The peak in concentration occurs between 25 and 50 mm downstream, just off the centerline. The levels are less than the stoichiometric levels, indicating that the reaction is lean.

**3.1.3 Flux of vapor** The vapor concentration measurements can be combined with the gas phase velocity measurements to provide the flux of vapor at each point. In the non-reacting case, this can be done with high accuracy since the conversion from mole fraction to mass fraction can be made without significant assumptions about the mixture molecular weight in the case of methanol. In the reacting case, enhanced vapor production is offset by consumption, so the vapor flow rate is ambiguous in this case. As a result, these results are not presented here.

Figure 11 presents these combined results for the non-reacting case. Figure 11a shows the evolution of the radial profiles of the vapor mass flux. The recirculation zone downstream of the atomizer causes the negative flux at the centerline at

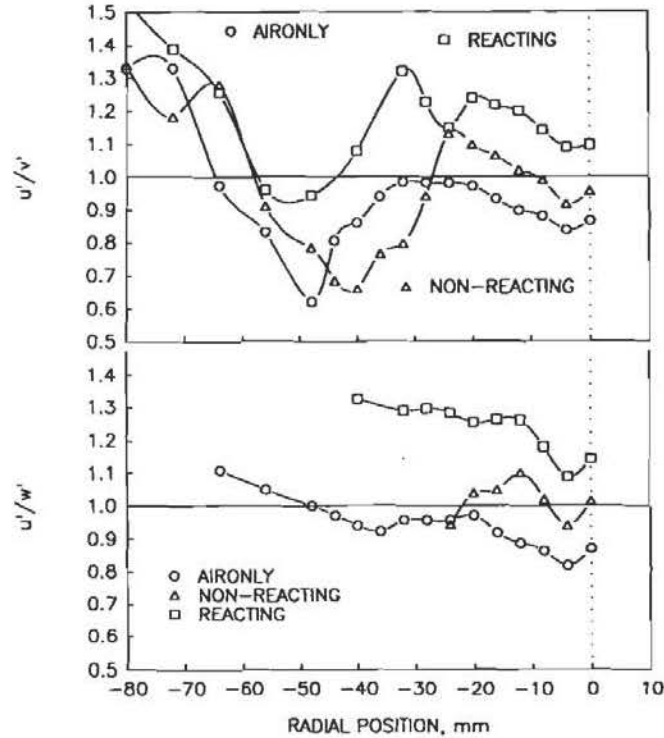


FIGURE 8 Comparison of  $u'$ ,  $v'$ , and  $w'$  at  $Z = 75$  mm.

$Z = 7.5$  mm. The decay of the recirculation zone results in local minima, but still in the positive direction, of the vapor flux. Since the concentration doesn't have strong gradients (Figure 9), the strong gradients in the flux are due largely to the velocity gradients. As a result, the extent of fluctuations in the vapor flux can be determined from the fluctuations in the velocities.

Integrating the profiles from Figure 11a in the radial and azimuthal direction leads to the results presented in Figure 11b, which presents the mass flow rate of vapor as a function of axial distance. Recalling that 1.26 g/s of methanol was initially injected, the results show that about one third of the spray has vaporized by  $Z = 100$  mm. Measurement of the flux of vapor has proven to be less susceptible to errors than is the measurement of the flux of liquid via PDI (e.g., McDonell and Samuelsen, 1991b), especially in complex flows such as the present one. The errors shown are based upon use of  $U$  from orthogonal radial traverses, and indicates the degree of symmetry in the axial velocity field. Measurement of the vapor concentration for different atomizer rotational positions indicated variations of less than 10% at any given radial location.

### 3.2 Droplet Behavior

Measurements of the droplets provide the size distributions at each location, along with coincident measurement of the velocity of each droplet. Data are acquired in the radial direction until the point where the measured liquid flux is 1% of the maximum flux along the profile. The results for the droplets are presented in terms of distribution means and size-velocity relationships.



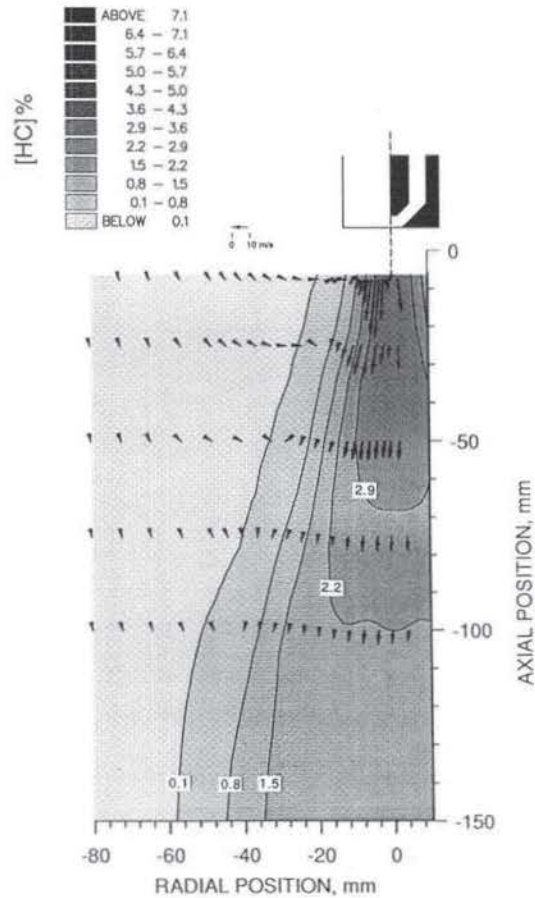


FIGURE 9 Contours of  $[HC]$  and gas phase velocity vectors in the  $r$ - $Z$  plane for the non-reacting case.

3.2.1  $D_{10}$ ,  $D_{32}$  The distribution number mean and Sauter Mean diameters,  $D_{10}$  and  $D_{32}$ , are presented in Figure 12 for both the reacting and non-reacting cases. At  $Z = 15$  mm, only small differences are observed between the two cases as expected. Farther downstream, greater differences are observed, especially near the edge of the spray, with both means being lower for the reacting case. This implies that reaction tends to reduce the size of all drops significantly for this case. Unfortunately, in this case, it is difficult to separate the effects of evaporation and transport of the drops, as might be done in the case without swirl (McDonell *et al.*, 1991b).

However, this same type of consistent decrease in the distribution means has been observed previously in other types of sprays operated under reacting and non-reacting conditions (e.g., McDonell and Samuelsen, 1991b; McDonell *et al.*, 1991b). In principle, it is possible for the mean size to increase due to preferential vaporization of small drops (e.g., Chin *et al.*, 1984), but in the studies considered in Table I, this behavior has only been observed experimentally by Bachalo *et al.*, 1990. Other researchers have found both increases and decreases in the distribution means for different regions of the spray (e.g., Mao *et al.*, 1986; Hardalupus, Taylor, and Whitelaw, 1990; McDonell, Wood, and Samuelsen, 1986). Ambiguity arises in a few of the above studies due to

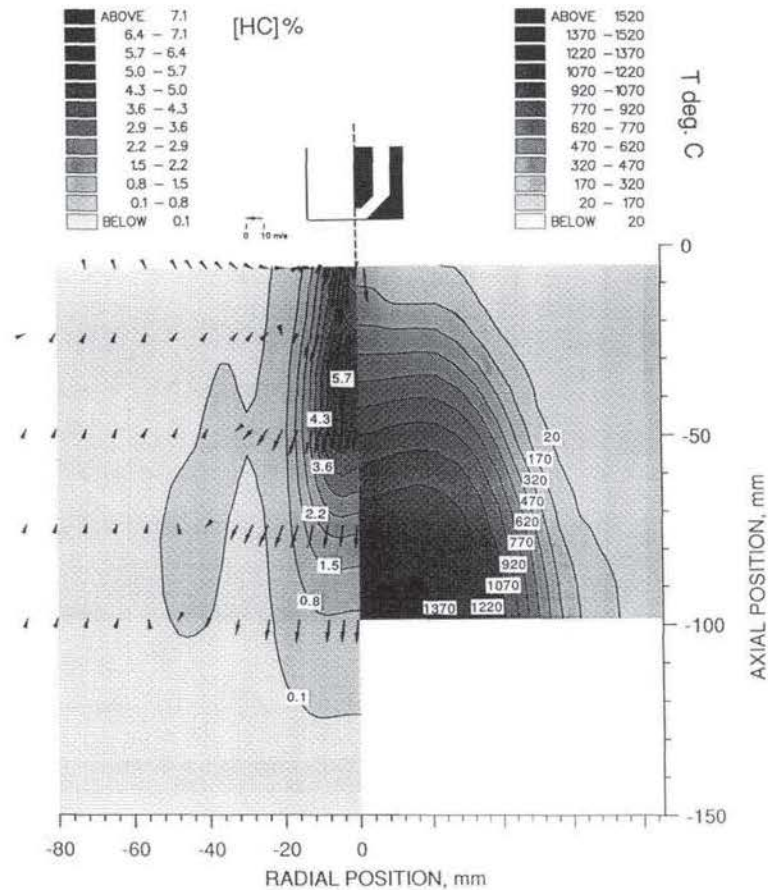


FIGURE 10 Contours of  $[HC]$ ,  $T$ , and gas phase velocity vectors in the  $r$ - $Z$  plane for the reacting case.

the presence of aerodynamic swirl (McDonell *et al.*, 1986; Bachalo *et al.*, 1990; Hardalupus *et al.*, 1990) which further couples evaporation and droplet transport in determining the local distribution means. Further complexity is added as a result of strong size-velocity correlations, which makes it difficult to establish a result for the entire spray because of the variation in time scales associated with each size class.

**3.2.2 Drop size velocity relationship** To better understand the transport of different size classes, Figure 13 presents a comparison of  $U$ ,  $V$ , and  $W$  for different size classes. For reference, the velocity of the gas phase is also presented as previously shown in Figures 2–4. In general, the reacting case exhibits a size-velocity correlation which persists farther downstream than does the non-reacting case. One challenge in the comparison is the lack of knowledge of where each drop represented came from. For example, a large drop in the non-reacting case at  $Z = 25$  mm will remain large at  $Z = 75$  mm. The same drop in the reacting case, however, will be significantly smaller at  $Z = 75$  mm. Hence, a drop measured as  $68 \mu\text{m}$  at  $Z = 75$  mm for the two cases will have had a much different life history. Similar size-velocity behavior was observed in both McDonell and Samuelsen (1991b) and Hardalupus *et al.* (1990). McDonell

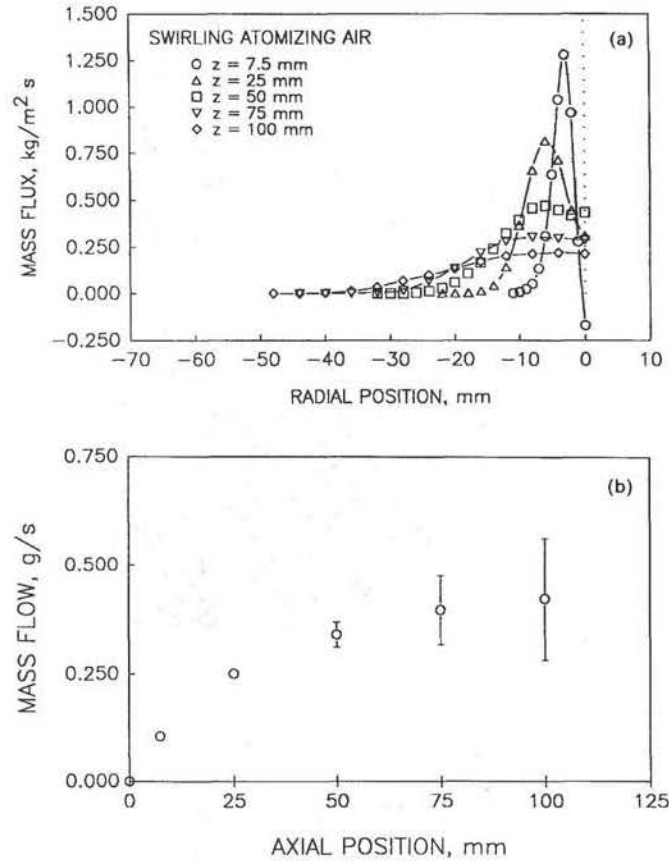
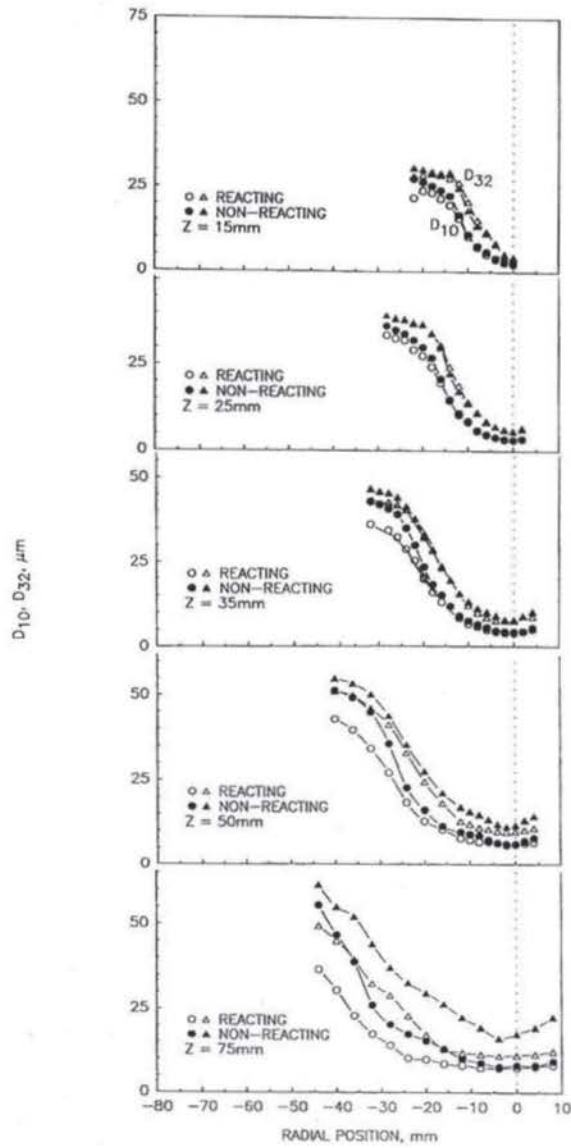


FIGURE 11 Vapor mass flux for the non-reacting case.

and Samuelsen (1991b) provide a similar explanation for this observation. Hardalupus *et al.* (1990) also provide similar reasoning for the observed differences, but also reason that slow moving drops vaporize within the recirculation zone, thus not contributing low velocities that they would provide in the non-reacting case. Again, the differences in geometry make generalization difficult.

An example of this is shown in Figure 13a which presents radial profiles of the mean axial velocity as a function of drop size,  $U(D)$ , for the two cases. In the non-reacting case, by  $Z = 75$  mm, the relative velocity between size classes is much less than it is at  $Z = 25$  mm. At the centerline, variation in velocity among size classes results in the increase in the gas phase fluctuating velocities as shown in Figure 5. In the reacting case, the relative velocities remain quite high at  $Z = 75$  mm. This occurs because a  $68 \mu\text{m}$  drop at  $Z = 75$  mm in the reacting case must have been much larger at  $Z = 25$  mm.

Figure 13b presents radial profiles of  $V(D)$ . Note that the largest drops have the highest radial velocities. Hence, only the largest drops possess enough momentum to overcome the inward force imposed by the atomizing air and entrained air. Interestingly, the  $15 \mu\text{m}$  drops do not reflect the large velocities away from the centerline shown by the gas phase until well downstream of the atomizer. Further examination of the droplet size velocity correlation at  $r = 4$  and  $8$  mm at  $Z = 25$  mm reveals that,

FIGURE 12 Radial profiles of  $D_{10}$  and  $D_{32}$ .

although the drops present there are all less than  $30\ \mu\text{m}$ , a strong size velocity correlation exists at these locations. The correlations show that the smallest drops do follow the gas phase radial velocities and that the radial velocity of the drops decreases consistently with drop size. The reason for this behavior is not clear. Values of  $u'$  for drops of this size and the gas phase are approximately the same, so random trajectories associated with the small drops does not appear to be responsible for this observation. Apparently, the way in which the air impinges upon the liquid sheet virtually eliminates the radial momentum of the  $15\ \mu\text{m}$  drops, while the pressure field



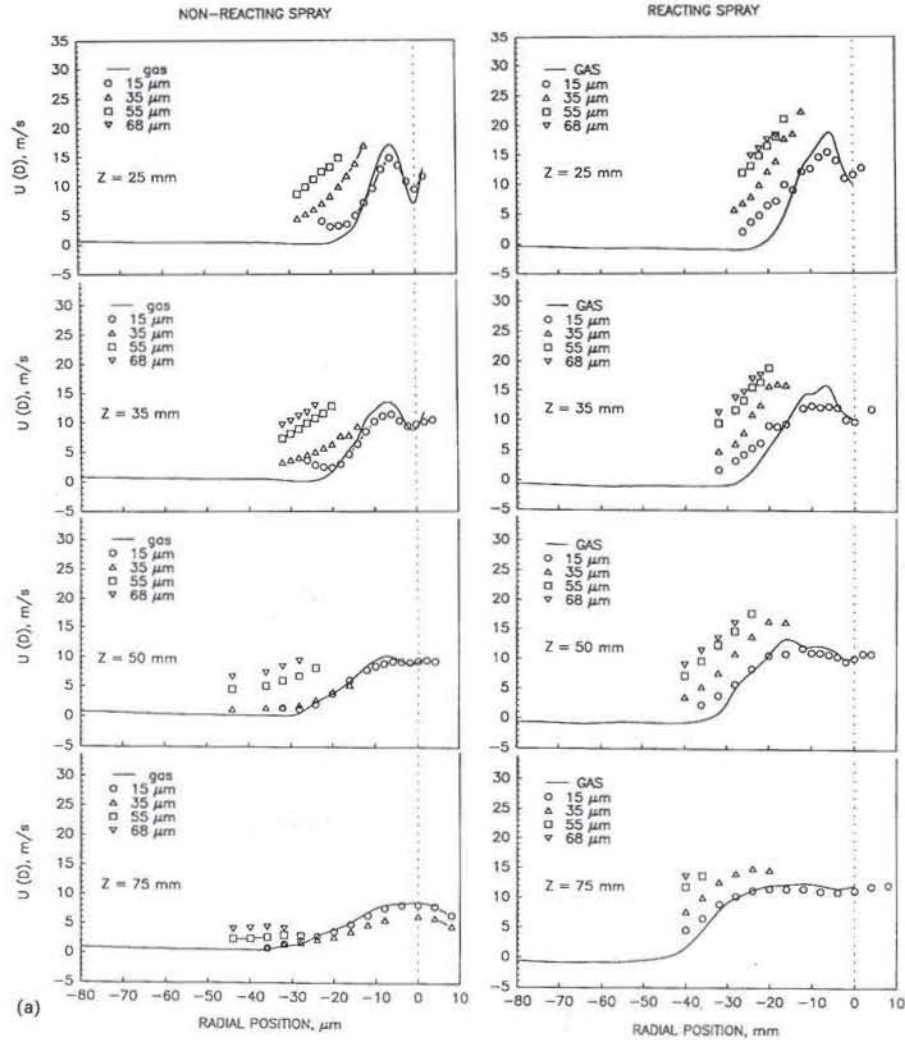


FIGURE 13 Comparison of  $U(D)$  for non-reacting and reacting cases. (b) Comparison of  $V(D)$  for non-reacting and reacting cases. (c) Comparison of  $W(D)$  for non-reacting and reacting cases.

established causes significant radial velocities to occur in the gas phase. Additional studies are needed to better understand this behavior. Of the studies shown in Table I, that of Mao *et al.* (1986) and McDonnell *et al.* (1986), are similar enough in atomizer type (twin-fluid, with swirling atomizing air) to provide comparison, but neither provides measurements of the radial velocity.

Figure 13c presents radial profiles of  $W(D)$ . In this case, by  $Z = 25$  mm, all the drops have attained swirling velocities similar to the gas phase. That even the smallest drops lag the gas phase in the regions of highest  $W_{\text{gas}}$  is not surprising since all tangential momentum possessed by the drops is due to the atomizing air. No strong size-azimuthal velocity correlation is observed, but it is likely that the impact of the atomizing air swirl tends to centrifuge drops away from the centerline, augmenting the

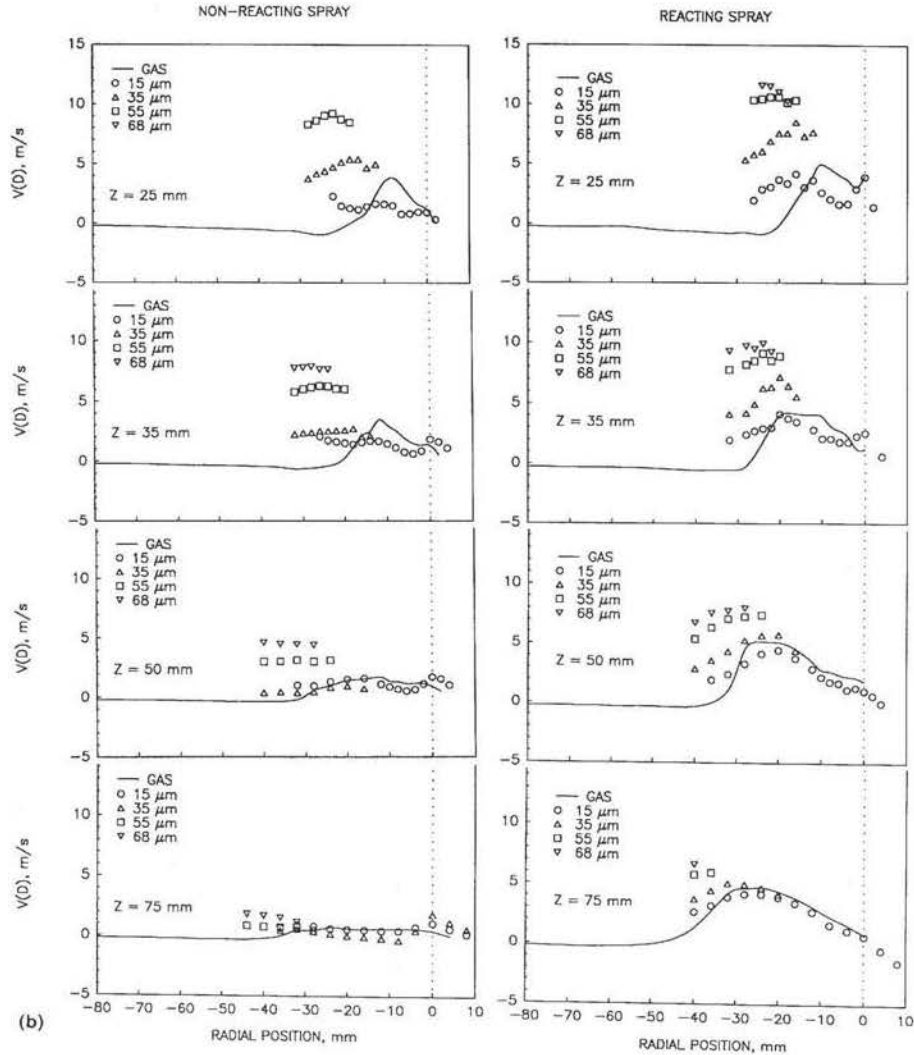


FIGURE 13 Continued.

already higher levels of radial momentum of the largest drops. Similar results were observed by Hardalupus *et al.* (1990), despite the differences in the flow geometry. In their case, however, stronger dependence of  $W$  upon  $D$  is observed, which is associated with the presence of aerodynamic swirl in their case. They did not, however, provide  $W(D)$  for the reacting case.

McDonell and Samuelsen (1991b) do not show  $W(D)$ , but state that no strong dependence of  $W$  on  $D$  is observed, which is consistent with the present study. The role of atomizing air swirl vs aerodynamic swirl appears differently in the azimuthal velocity dependence upon  $D$  based on the comparisons of the present case and that of Hardalupus *et al.* (1990).

Droplet fluctuating velocities are not presented here for brevity, but are available (McDonell and Samuelsen, 1990). Essentially, these results indicate that the fluctuat-

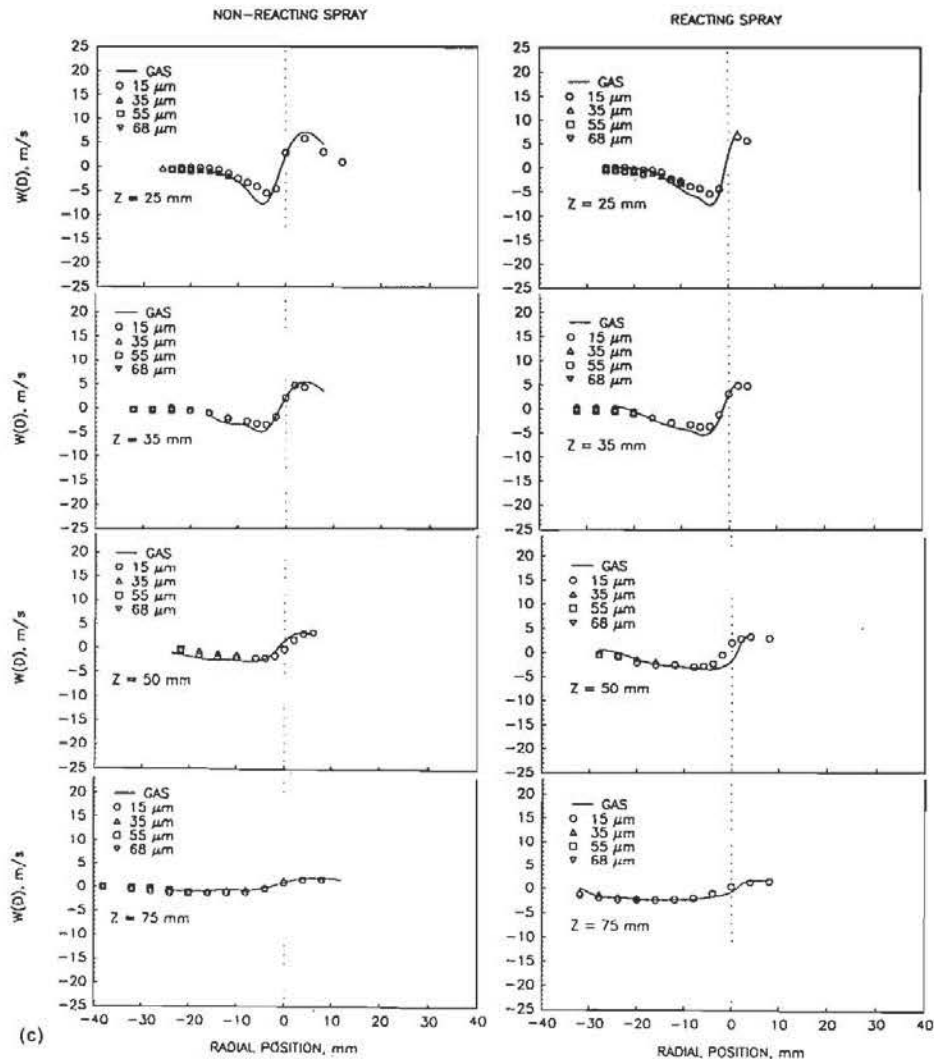


FIGURE 13 Continued.

ing velocities of the large drops are less than those of the small drops at most locations: This is consistent with observations of Hardalupus *et al.* (1990). The fluctuating velocities of the gas phase is not necessarily less than or greater than that of the droplets. This is difficult to interpret because the fluctuating velocities of the drops are due to superposition of velocity variations due to (1) variation in drop origination, and (2) variation imparted by the gas phase turbulence. In the former case, the variation in the aerodynamic effects on drops arriving from different locations can cause a relatively large variation in the measured velocity at a given point.

**3.2.3 Droplet dynamics** The time averaged structure of the spray has been presented thus far. However, the instantaneous behavior is also important to understand, especially in terms of local mixing effectiveness. Figure 14 presents maps of the droplet



size vs time measured at different points in the spray. The axis labels shown in the lower left plot are the same for each location. The sections of the time series shown are representative of the droplet dynamics at each of the points.

Figure 14a presents the map for the non-reacting case. In this case, the abscissa scale is condensed by a factor of 10 from that of the reacting case (Figure 14b). FFT's of these time series showed no strongly dominating frequency, indicating that the drops arrive in essentially random fashion. Figure 14a indicates that, near the centerline, the drops arrive in a consistent manner, with no large time gaps between droplets. Farther from the centerline (*e.g.*,  $Z = 50$  mm,  $r = 16$  mm;  $Z = 75$  mm,  $r = 24$  mm), more variation in the time between drops is observed with more pronounced voids and clusters of drops.

Figure 14b shows the same type of map for the reacting case. Here, the impact of reaction is evident, especially when comparing the  $Z = 50$  mm locations to the  $Z = 75$  mm locations. It is difficult to see any structure at the centerline due to the time scale compression, but like the non-reacting case, drop arrival is more consistent than it is at the edge of the spray. At  $Z = 75$  mm, the voids present in the reacting case are increased compared to those in the non-reacting case, with even more time when no drops are present. This type of droplet arrival leads to local variation in stoichiometry which is not desirable for either stability or emissions characteristics.

Time resolved measurements are important to have when examining the local structure of the spray. More work is required to correlate the clustering with either atomization or aerodynamics or other factors. Recent numerical studies indicate that the clustering can be directly caused by the aerodynamics of the flow (*e.g.*, Squires and Eaton, 1990).

#### 4 SUMMARY

A detailed characterization of a swirling air-assisted spray has been conducted. This study reflects one part of a study which removes fuel type, geometry, and stoichiometry from the list of variable, and concentrates on the role of the atomizer type. Where possible, results from this study are compared to the findings of other studies which provide spatially resolved measurements in reacting sprays. The comparison of results indicate that (1) only a small number of data sets are available against which to compare the current results, and (2) consistency between data sets has not yet been reached. The majority of the studies do find that (1) droplets modulate the gas phase mean and fluctuating properties in a complex fashion, (2) the drops have less impact on the swirling component of velocity than on the radial or axial components, (3) reaction causes large increases in axial and radial velocities, and (4) the presence of reaction tends to increase the local drop size distribution means at the locations where measurements were obtained. Also, it is evident that the complexity of spray flames will require additional studies such as the present one to separate system specific effects.

For the present spray, the following observations have been made:

- The present of drops alters the structure of the turbulence of the gas phase, including the degree of isotropy.
- The presence of reaction accelerates the gas phase in the axial and radial directions while having little impact on the amount of swirl in the flow. The presence of reaction causes the values of  $u'/v'$  and  $u'/w'$  to increase which is attributed in part to unsteadiness associated with the downfired orientation.
- Measurements of the vapor concentration show that saturated levels are reached

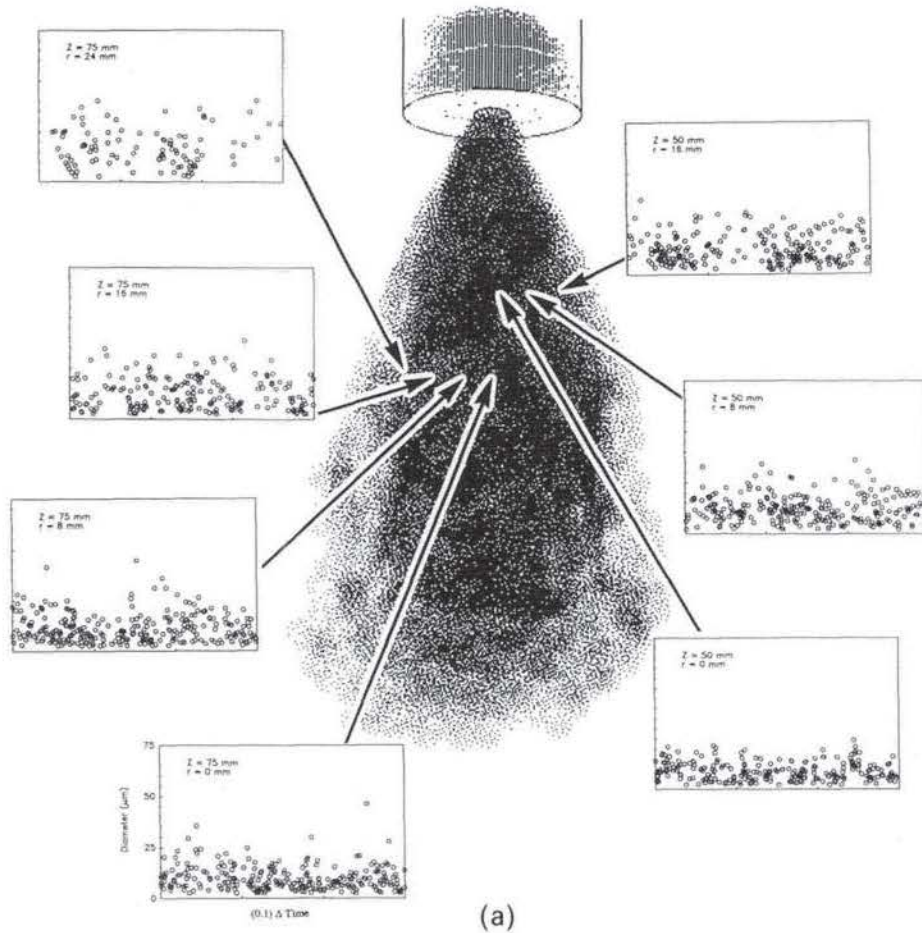


FIGURE 14 (a) Time-resolved measurements in the non-reacting spray. (b) Time-resolved measurements in the reacting spray.

immediately downstream of the atomizer for the non-reacting case, which is due to the rapid evaporation of small drops and the intense mixing in this region. Entrainment dilutes the peak levels of vapor at locations farther downstream.

- Reaction rapidly consumes the vapor, but the presence of intermittent large drops combined with the convection of hot products upstream cause local pockets of vapor at the edge of the spray. This behavior is consistent with photographs which show drops persisting at radial locations which are beyond the location of the apparent reaction zone. The peak levels of hydrocarbons in the reacting case reflect a lean reaction.
- The presence of reaction reduces the mean size of the drops at most locations, indicating that the rapid vaporization of small drops which would initially give rise to an increase in the mean size has been completed, and that significant vaporization has occurred for even the largest drops.
- Strong dependency of  $U$  and  $V$  on  $D$  is observed. Little or no dependency of  $W$  on  $D$  is observed. This is attributed to the near normal impact of the atomizing

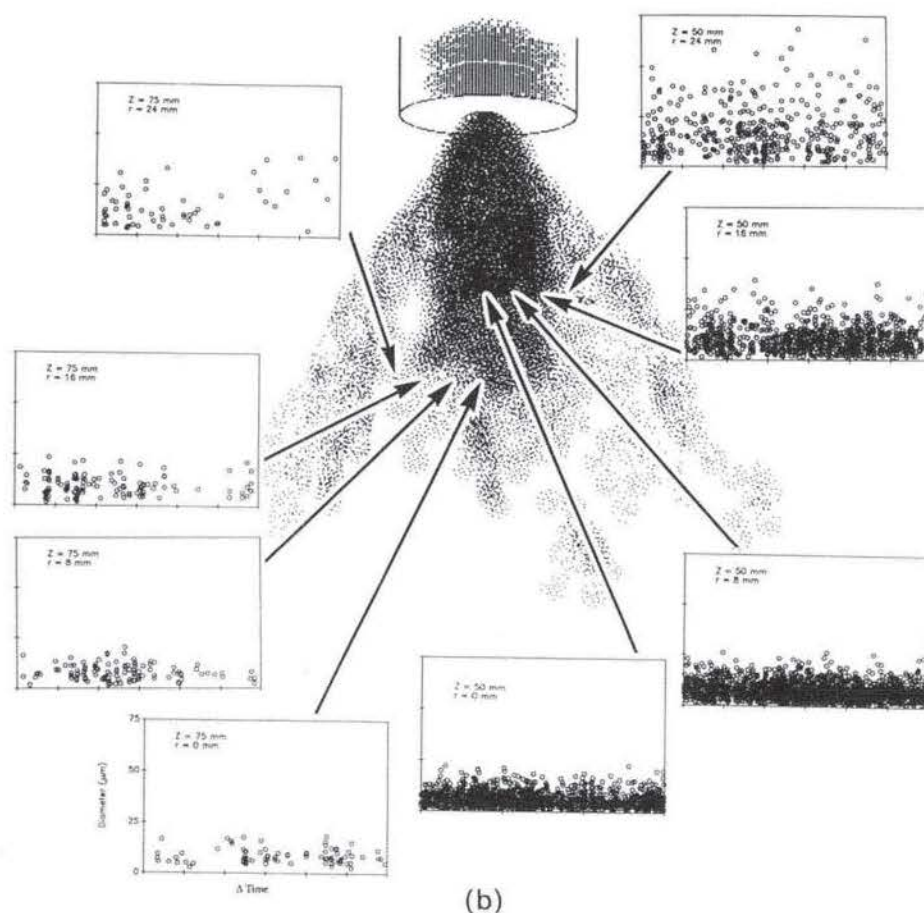


FIGURE 14 Continued.

air upon the liquid sheet, and the lack of swirl present in the fuel stream. In general, it is observed that the velocities of the drops exceeds that of the gas phase in the axial and radial direction, and that the velocity of the gas exceeds that of the drops in the azimuthal direction.

- Detailed examination of the local time resolved structure shows local clustering of drops for both non-reacting and reacting cases. More work is needed to determine if the clustering is due to atomization or associated with aerodynamics.

#### ACKNOWLEDGEMENTS

The authors would like to acknowledge the support of the Parker Hannifin Corporation for studies in the behavior and characterization of sprays and two-phase transport. In addition, an Air Force Laboratory Graduate Fellowship is gratefully acknowledged for the support of the principal author (VGM) and the support of Horiba, Ltd. for the participation of one of the authors (MA). The assistance of Susan Brockschmidt, and undergraduate student in mechanical engineering, in the reduction data and preparation of figures is appreciated.

## REFERENCES

- Adachi, M., McDonell, V. G., and Samuelsen, G. S. (1990). Non-intrusive measurement of gas species in reacting and non-reacting sprays. *Combustion Science and Technology* **75**, 179.
- Bachalo, W. D. and Houser, M. J. (1984). Phase Doppler spray analyzer for simultaneous measurements of drop size and velocity distributions. *Opt. Engr.* **23**, 583.
- Bachalo, W. D., Rudoff, R. C., and Sankar, S. V. (1990). Time-resolved measurements of spray drop size and velocity. *Liquid Particle Size Measurement Techniques: 2nd Volume*, ASTM STP 1083, E. D. Hirtleman, W. D. Bachalo and Philip G. Felton eds., ASTM, Philadelphia, PA 209-224.
- Chin, J. S., Durrett, R., and Lefebvre, A. H. (1986). The interdependence of spray characteristics and evaporation history of fuel sprays. *ASME J. Engr. Gas Turbines Power* **106**, 639.
- Chiu, H. H. and Liu, T. M. (1977). Group combustion of liquid droplets. *Combustion Science and Technology* **17**, 127.
- Hardalupus, Y., Taylor, A. M. K. P., and Whitelaw, J. H. (1990). Velocity and size characteristics of liquid-fuelled flames stabilised by a swirl burner. *Proceedings of the Royal Society of London Series A—Mathematical and Physical Sciences* **428**, 129.
- Mao, C.-P., Wang, G., and Chigier, N. A. (1986). An experimental study of air-assist atomizer spray flames. *Twenty First Symposium (International) on Combustion*, The Combustion Institute, Pittsburgh, PA, 665-673.
- McDonell, V. G., Wood, C. P., and Samuelsen, G. S. (1986). A comparison of spatially-resolved drop size and drop velocity measurements in an isothermal chamber and a swirl stabilized combustor. *Twenty First Symposium (International) on Combustion*, The Combustion Institute, Pittsburgh, PA, 685-694.
- McDonell, V. G. and Samuelsen, G. S. (1991a). Structure of vaporizing pressure atomized sprays, submitted to *Atomization and Sprays*.
- McDonell, V. G. and Samuelsen, G. S. (1991b). Gas and drop behavior in reacting and non-reacting air-blast atomizer sprays. *AIAA J. of Propulsion and Power* **7**, 684.
- McDonell, V. G. and Samuelsen, G. S. (1990). Detailed data set: PDI and IRES measurements in methanol sprays under reacting and non-reacting conditions. UCI Technical Report ARTR-90-5 Part C: swirling air-assisted spray.
- McDonell, V. G., Adachi, M. A., and Samuelsen, G. S. (1991a). Structure of non-swirling air-assisted sprays under reacting and non-reacting conditions, Part I: gas phase behavior, submitted to *Atomization and Sprays*.
- McDonell, V. G., Adachi, M. A., and Samuelsen, G. S. (1991b). Structure of non-swirling air-assisted sprays under reacting and non-reacting conditions, Part II: drop behavior, submitted to *Atomization and Sprays*.
- Squires, K. D. and Eaton, J. K. (1990). Particle response and turbulence modification in isotropic turbulence. *Physics of Fluids A* **2**, 1191.